Available online at www.sciencedirect.com
SCIENCE DIRECT®
Journal of Solid State Chemistry 179 (2006) 341–348
JOURNAL OF SOLID STATE CHEMISTRY
www.elsevier.com/locate/jssc

An electron diffraction and bond valence sum investigation of oxygen/fluorine ordering in $Nb_nO_{2n-1}F_{n+2}$, $n = 3$

Frank J. Brink[a,*], Ray L. Withers[a], Stéphane Cordier[b], Marcel Poulain[b]

[a]*Research School of Chemistry, The Australian National University, Canberra, ACT 0200, Australia*
[b]*Laboratoire de Chimie du Solide et Inorganique, UMR 6511 CNRS-Université de Rennes1, Institute de Chimie de Rennes, Avenue du Général Leclerc, 35042 Rennes Cedex, France*

Received 4 July 2005; received in revised form 12 October 2005; accepted 16 October 2005
Available online 21 November 2005

Abstract

The $n = 3$ member of the $Nb_nO_{2n-1}F_{n+2}$ family of oxyfluoride compounds has been carefully investigated by electron diffraction. This compound was previously believed to have a random distribution of oxygen and fluorine ions at each of the anion sites. Electron diffraction experiments have revealed the presence of strong planar diffuse scattering perpendicular to the **a** and **b** directions at the $\mathbf{G}\pm[qkl]^*$ and $\mathbf{G}\pm[hql]^*$ regions of reciprocal space, where **G** represents a Bragg reflection of the $I4/mmm$ average structure, h and k are continuous variables and $q = 0.39 \pm 0.08$. The continuous planes of diffuse intensity imply the existence of strings of ordered oxygen and fluorine atoms for equatorial anion sites along [100] and [010] albeit without correlation from one such string to the next. A bond valence sum argument has been used to derive a plausible site occupation model for the remaining apical and median anion sites.

Keywords: Oxygen fluorine ordering; Diffuse scattering

1. Introduction

$Nb_3O_5F_5$ is the $n = 3$ member of an $Nb_nO_{2n-1}F_{n+2}$ ($1 \leqslant n \leqslant \infty$) homologous series of oxyfluoride compounds [1,2] (see Fig. 1a). One extreme end-member compound, NbO_2F ($n = \infty$), is of ReO_3 average structure type (space group symmetry $Pm\bar{3}m$) consisting of an infinite three-dimensional array of corner-connected NbX_6 (X = anion) octahedra [3–5] (see Fig. 1c). The average structures of each of the other members of this family of oxyfluoride compounds consist of two-dimensional slabs of NbO_2F regularly stacked on top of one another along the c direction, each slab being n octahedral layers thick and exhibiting a relative "shear-type" displacement of $(\frac{1}{2}\mathbf{a}+\frac{1}{2}\mathbf{b})$ on moving from one NbO_2F type slab to the next (see, e.g. Figs. 1a and b). The resultant unit cell of the finite n members of this family of compounds is thus body centered tetragonal (space group symmetry $I4/mmm$) in each case, with a largely constant a-axis dimension and a c-axis dimension that roughly scales as $2n$ times the cubic unit cell dimension of NbO_2F ($a = 3.902$ Å). Thus $a = 3.914(1)$ Å, $c = 24.211(1)$ Å for $Nb_3O_5F_5$ ($n = 3$) while $a = 3.953(1)$ Å, $c = 8.359$ Å for $NbOF_3$ ($n = 1$), etc. (see Figs. 1a and b).

Recent structural investigations of the $n = 1$, 3, and ∞ members of this $Nb_nO_{2n-1}F_{n+2}$ family of compounds [1,2,5] have come to quite differing conclusions as regards O/F ordering therein. In a recent study of $Nb_3O_5F_5$ [1], for example, there was reported to be no evidence for O/F ordering. Each of the four available anion sites (for $I4/mmm$ space group symmetry) were reported to have a 50/50 (i.e. a statistical) distribution of O and F ions (see Table 1 and Ref. [1]). In the case of $NbOF_3$ [2], it was suggested that there is some (indirect) evidence for a preferential distribution of O and F onto the two available anion positions. This is not however quantified. The authors only state that the equatorial anion sites are likely to be "…more favorable…" for an O^{2-} ion while the apical anion sites could "…more reasonably…" be expected to be occupied by a F^- ion. Rietveld refinement also suggests

*Corresponding author. Electron Microscope Unit, Research School of Biological Sciences, Australian National University, Canberra, ACT 0200, Australia. Fax: +61 2 6125 3218.
E-mail address: brink@rsbs.anu.edu.au (F.J. Brink).

0022-4596/$ - see front matter © 2005 Elsevier Inc. All rights reserved.
doi:10.1016/j.jssc.2005.10.014

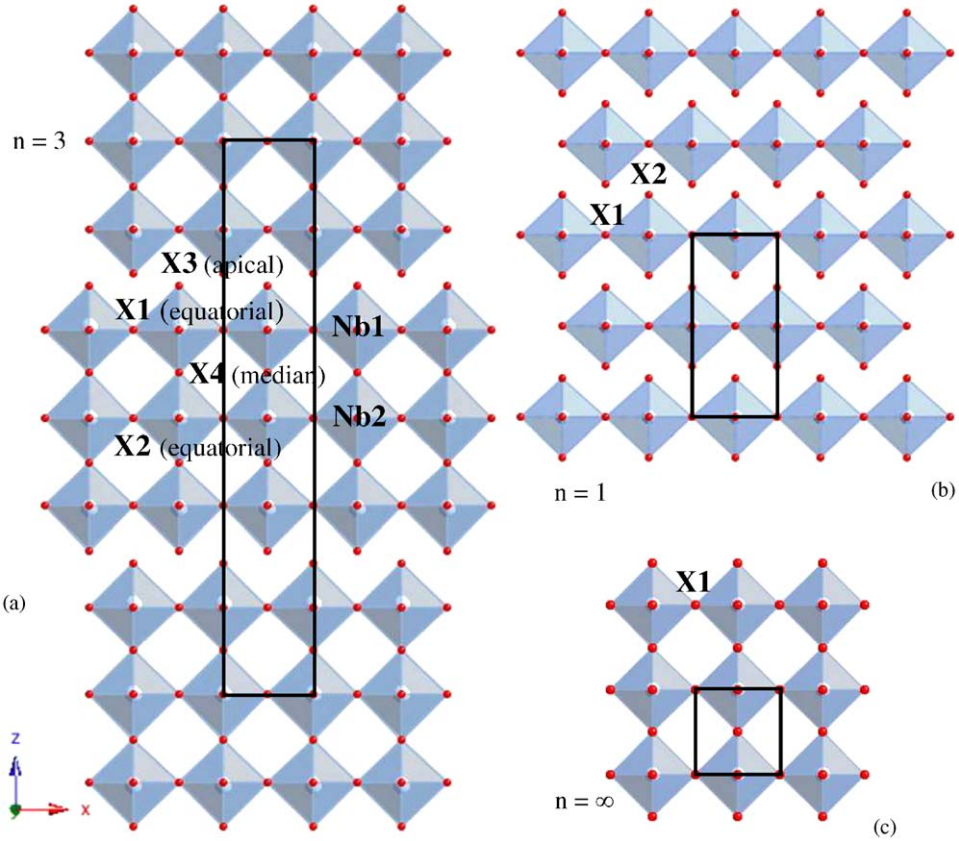

Fig. 1. Diagram showing the stacking arrangement for the $n = 1$, 3, and ∞ members of the $Nb_nO_{2n-1}F_{n+2}$ family of oxyfluoride. The unit cell is outlined in each case.

Table 1
Wyckoff positions and site occupancies for the refined average structures of $Nb_3O_5F_5$ [1] and $NbOF_3$ [2]

Atom	Wyckoff site	x	y	z	Occupancy
$Nb_3O_5F_5$ space group $I4/mmm$ (No. 139): $a = 3.9135(1)$ Å, $c = 24.2111(2)$ Å					
Nb1	4*e*	0	0	0.1638(2	1
Nb2	2*a*	0	0	0	1
*X*1	8*h*	1/2	0	0.1589(9)	0.5O, 0.5F
*X*2	4*c*	0	1/2	0	0.5O, 0.5F
*X*3	4*e*	0	0	0.2390(9)	0.5O, 0.5F
*X*4	4*e*	0	0	0.0811(9)	0.5O, 0.5F
$NbOF_3$ space group $I4/mmm$ (No. 139): $a = 3.9675(1)$Å, $c = 8.4033(1)$Å					
Nb1	2*a*	0	0	0	1
*X*1	4*c*	1/2	0	0	0.275O, 0.725F
*X*2	4*e*	0	0	0.2196(1)	0.225O, 0.775F

that O has a preference for the equatorial *X*1 anion site although the reported degree of O/F ordering is minimal (see, e.g. Table 1 and Ref. [2]). On the other hand, a recent electron diffraction investigation of the $n = \infty$ end-member compound NbO_2F [5] found clear evidence for one-dimensional (⋯–O–O–F–O–O–F–⋯) O/F ordering along each of the real space $\langle 001 \rangle$ directions in the form of planes of diffuse intensity running through the $\mathbf{G} \pm \langle hk\frac{1}{3} \rangle^*$ (**G** a parent Bragg reflection, h and k continuous variables) regions of reciprocal space.

Given the strong evidence for one-dimensional O/F ordering in NbO_2F and the close structural relationship between NbO_2F and the other members of the $Nb_nO_{2n-1}F_{n+2}$ family of compounds, it seemed highly unlikely that O/F ordering should not also be characteristic of the latter family of compounds. It was therefore decided to carry out a detailed electron diffraction and bond valence sum investigation of the $n = 3$ compound $Nb_3O_5F_5$ again looking for evidence of O/F ordering.

2. Synthesis and data collection

$Nb_3O_5F_5$ was obtained according to the procedure described in Ref. [1] starting from NbO_2F and NbF_5 precursors. NbO_2F (770 mg) and an excess of NbF_5 (395 mg) were weighed, ground and pelleted in a controlled atmosphere glove box. It was then introduced into a nickel container that was subsequently welded under argon and encapsulated in an evacuated silica ampoule. After two weeks heating at 240 °C, the tube was opened and the excess of NbF_5 eliminated at 120 °C under dynamic vacuum. The final product was obtained as a blueish powder, which is stable in air. X-ray powder diffraction analysis revealed the presence of less than 5% non reacted NbO_2F in the final $Nb_3O_5F_5$ sample.

Electron probe microanalysis (EPMA) was used to to determine composition. Samples were prepared by mounting the prepared powder in resin followed by polishing to a $<0.5\,\mu m$ finish. The analyses were carried out using wavelength dispersive spectrometry (WDS) at 8 kV and 30 nA in a Cameca SX 50. The system was calibrated using $LiNbO_3$ as a reference standard for O and Nb and Topaz for F. The final result was based on the average and standard deviation of 30 point analyses taken on individual grains. The composition of the grains was found to be homogeneous and in rather good agreement ($Nb_{3.07(5)}O_{5.08(9)}F_{4.92(8)}$) with the expected $Nb_3O_5F_5$ stoichiometry.

Samples suitable for transmission electron microscopy (TEM) were prepared by the dispersion of finely ground material onto holey carbon coated copper grids. Electron diffraction patterns (EDPs) were obtained using a Philips 430 TEM.

3. Electron diffraction results

Given the earlier evidence (in the form of a highly structured diffuse intensity distribution) for O^{2-}/F^- ordering in NbO_2F, electron diffraction has again been employed to search for similar weak features of reciprocal space indicative of O^{2-}/F^- ordering in $Nb_3O_5F_5$. These diffraction experiments revealed striking similarities, but also some differences, to the previously investigated NbO_2F. The reciprocal lattice of $Nb_3O_5F_5$ is again characterized by the presence of sheets of diffuse intensity, but now restricted to directions perpendicular to [100] and [010] at the $\mathbf{G}\pm[qkl]^*$ and $\mathbf{G}\pm[hql]^*$ regions of reciprocal space (q fixed, h, k, and l continuously variable). Evidence for this can be seen in Figs. 2a and b which show $[1\bar{1}1]$ and $[2\bar{1}1]$ zone axis EDPs of $Nb_3O_5F_5$. The presence of strong, transverse polarized, lines of diffuse streaking running along the $[10\bar{1}]^*$ and $[011]^*$ directions of reciprocal space in Fig. 2a is immediately apparent. As we continue tilting along the $[011]^*$ systematic row this diffuse streaking continues to be present until we arrive at the $[2\bar{1}1]$ zone axis orientation by which stage the diffuse streaking runs along the $[10\bar{2}]^*$ and $[011]^*$ directions of reciprocal space (see Fig. 2b).

In general the diffuse streaking is always observed to run along the $[h0l]^*$ and $[0kl]^*$ directions of reciprocal space, which can only be interpreted in terms of planes of diffuse intensity orthogonal to each of the **a** and **b** crystal directions. As was observed for NbO_2F, it is also clearly evident that the intensity of the diffuse streaking has a very strong angular, or azimuthal, dependence and there is again a large size effect type redistribution of diffuse intensity from the low to the high angle side of the parent Bragg reflections [5–7] (see, e.g. the apparent absence of streaking on the low angle side of the parent Bragg reflections at $\mathbf{G}-[qkl]^*$ and $\mathbf{G}-[hql]^*$, respectively, in Fig. 2). Such behavior is directly analogous to that observed for NbO_2F [5] and suggests large amplitude cation displacements induced by the local O/F distribution are again responsible for the observed diffuse distribution.

Fig. 3a shows an EDP of $Nb_3O_5F_5$ taken at a [100] zone axis orientation. (The layered nature of $Nb_nO_{2n-1}F_{n+2}$

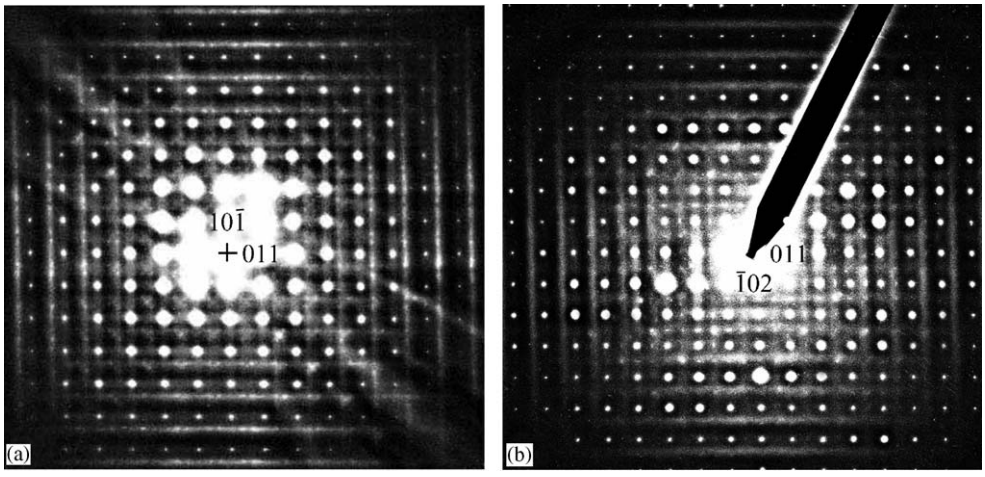

Fig. 2. Shows typical (a) $[1\bar{1}1]$ and (b) $[2\bar{1}1]$ zone axis EDPs for $Nb_3O_5F_5$. Each EDP displays strong essentially continuous, transverse polarized streaking along the $[h0l]^*$ and $[0kl]^*$ directions of reciprocal space.

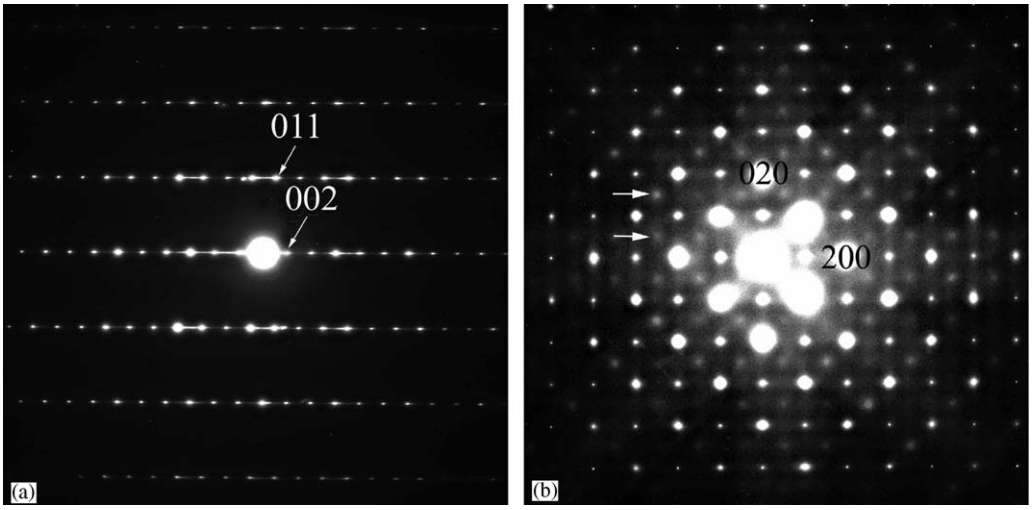

Fig. 3. Shows (a) a typical [100] zone axis EDP for $Nb_3O_5F_5$, note the sharp streaking through the [010]* position of reciprocal space. (b) A [001] zone axis EDP. The presence of space group forbidden [hk0]* ($h+k$ = odd) reflections as well as the presence of [$\frac{11}{22}\,\xi$] octahedral rotation modes (arrows) are clearly seen.

compounds ensures that they invariably cleave perpendicular to **c** meaning that EDPs with **c*** excited, such as Fig. 3a, are rather difficult to obtain from crushed crystal fragments). Note that the positioning of the strong parent Bragg reflections in this EDP are entirely consistent with the $I4/mmm$ average structure space group symmetry reported for $Nb_3O_5F_5$, i.e. $F(hkl)=0$ unless $h+k+l$ is even. In addition to these strong average structure Bragg reflections, however, note the sharp diffuse streaking running through the parent Bragg reflections along the c* direction of reciprocal space. The fact that this diffuse streaking is so sharp and that it runs through the undiffracted 0 0 0 beam strongly suggests that it arises as a result of (001) stacking fault disorder (cf. for example, with Fig. 1 of Ref. [8]), i.e. as a result of some local 'disorder' in the width of the NbO_2F slabs.

Such stacking fault 'disorder' locally destroys I-centering and gives rise to the apparent presence of the nominally space group forbidden [hk0]* ($h+k$ odd) Bragg reflections in the Zero Order Laue Zone (ZOLZ) region of the [001] zone axis EDP shown in Fig. 3b. The apparent presence of such space group forbidden reflections in Fig. 3b is entirely consistent with the diffuse streaking observed running through, e.g. the [010]* position in reciprocal space in the [100] zone axis EDP of Fig. 3a. Note that the presence of the nominally space group forbidden [hk0]* ($h+k$ odd) Bragg reflections in Fig. 3b cannot be attributed to octahedral rotation modes as occurs in the case of NbO_2F, as they do not occur at the $\mathbf{G}\pm[1/2,1/2,\xi]$* positions of reciprocal space characteristic of such modes.

Direct evidence for the existence of the latter Rigid Unit Mode (RUM) octahedral rotation modes in the case of $Nb_3O_5F_5$ can be found, however, in the presence of just such 'satellite reflections' (at the $\mathbf{G}\pm[1/2,1/2,\xi]$* positions of reciprocal space) in Fig. 3b. The positioning as well as the intensity distribution of these 'satellite reflections' shows that they are necessarily associated with octahedral rotation (RUM) modes of distortion, directly analogous to those observed in NbO_2F [5].

4. Interpretation and discussion

The clear diffraction evidence for planar sheets of transverse polarized, diffuse intensity at the $\mathbf{G}\pm[qkl]$* and $\mathbf{G}\pm[hql]$* regions of reciprocal space (q fixed, h, k, and l continuously variable) is entirely analogous to the structured diffuse distributions previously reported as characteristic of NbO_2F [5] and the $Nb^{V}_{1-x}Nb^{IV}_{x}O_{2-x}F_{1+x}$ solid solution field [9]. In the case of the latter $Nb^{V}_{1-x}Nb^{IV}_{x}O_{2-x}F_{1+x}$ solid solution field, the magnitude of the one-dimensional primary modulation wave-vector q was shown to be directly correlated with the O/F ratio along the $\langle 001 \rangle$ directions. Given the close structural relationship between the latter $Nb^{V}_{1-x}Nb^{IV}_{x}O_{2-x}F_{1+x}$ solid solution field and the current $Nb_3O_5F_5$ compound, one would therefore expect that q, the magnitude of the one-dimensional primary modulation wave-vector in the case of $Nb_3O_5F_5$, would again act as a 'chemical ruler' and be directly related to the O/F ratio—albeit this time only for the equatorial anion sites (the $X1$ and $X2$ anion sites) along the **a** and **b** directions (see Fig. 1a).

Careful measurements of scanned traces from the experimental EDPs of $Nb_3O_5F_5$ shown in Fig. 2 reveals that the diffuse sheets occur at $q\sim0.39\pm0.08$ (see Fig. 4), suggesting that the average anion composition along [100] and [010] anion strings must correspond to 0.39 F and 0.61 O i.e. the occupancy of the $X1$ and $X2$ equatorial sites are given by 0.39 F and 0.61 O. A reasonable model for the ordering sequence of O's and F's along these [100] and [010] directions can be obtained using an occupational crenel Atomic Modulation Function [9–11] and making the approximation $q\approx 2/5$ (see Fig. 5). The crenel function

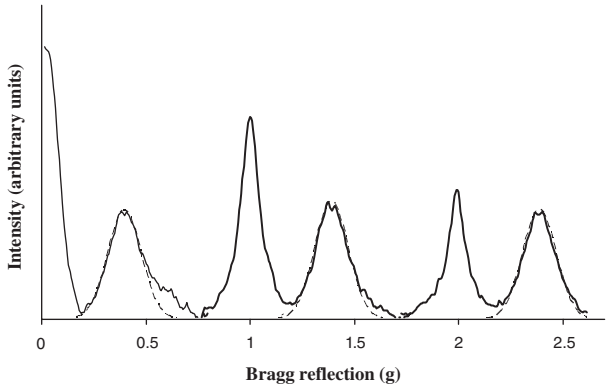

Fig. 4. This plot shows the average of 12 line profiles taken perpendicular to the diffuse streaking along the [011]* direction of reciprocal space. A normal distribution has been used to provide a fit to the line profile (dotted line) at positions of the diffuse distribution in order to obtain a more accurate estimate of the magnitude of the q vector.

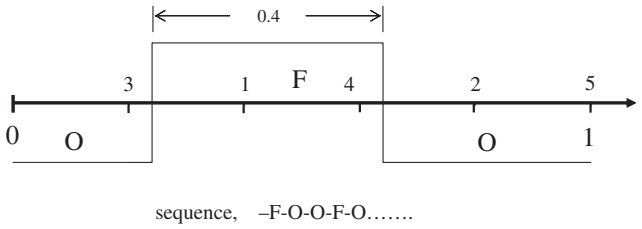

Fig. 5. Diagram showing the Crenel type function used to predict the O/F configurations along the [100] and [010] directions in Nb_3O_5F5.

runs along the x_4 ($\equiv qx$ modulo an integer) axis and is defined by two parameters, the crenel width, which is the F occupation interval (0.4) and the crenel midpoint (0.2). The predicted ordering sequence ⋯–|F–O–O–F–O|–F–O–⋯ is then simply generated by carrying out 5 translations of 2/5 along x_4.

Note that the observed diffuse distribution shown in Fig. 2 only gives information as to the O/F distribution along the infinite ⟨100⟩ and ⟨010⟩ anion strings and gives no information as to the O/F distribution along the strictly limited ⟨001⟩ anion strings, i.e. it contains no information as to the occupancies of the apical $X3$ and $X4$ sites. For this we turn to bond valence sum considerations using the published average structure refinement of Ref. [1].

4.1. Bond valence sum considerations

The bond valence sum method, an empirically based approach, has proven itself over many years to be extremely useful in investigating the local crystal chemistry and hence structural validity of many proposed crystal structures. In the case of disordered average structures, bond valence sum calculations have also proven to be very useful in predicting the sorts of local structural adjustments that are necessary in order to obtain reasonable local crystal chemistry.

In the case of NbO_2F, for example, it has been used to show how one-dimensional ⟨001⟩ O/F ordering (along with the associated induced cation and anion displacements) acting in concert with octahedral rotation (RUM) modes can give rise to a very significant improvement in local crystal chemistry [5]. From the bond valence point of view, NbO_2F represents a very simple case in that there is only one cation site and one anion site per average structure unit cell. In the case of $Nb_3O_5F_5$, the situation is rather more complex since we now have two symmetry inequivalent cation sites and four symmetry inequivalent anion sites per average structure unit cell (see Fig. 1a and Table 1). Nonetheless, we believe it remains quite possible to deduce the average site occupancies of the 4 symmetry inequivalent anion sites per average structure unit cell from the refined average structure fractional co-ordinates as follows.

Suppose that the individual fractional F site occupancies, x_i, at each of the symmetry inequivalent anion sites $X1$, $X2$, $X3$, $X4$ within the $Nb_3O_5F_5$ average structure are as follows:

$$x_iF + (1 - x_i)O, \quad i = 1 \text{ to } 4, \quad 0 \leqslant x_i \leqslant 1.$$

The formal Apparent Valence, AV(Xi), at each of the anion sites, Xi, should then be given by

$$\mathrm{AV}(Xi)_{(\mathrm{ideal})} = x_i(1) + (1 - x_i)(2) = 2 - x_i.$$

Using the refined Nb-anion bond distances taken from the X-ray diffraction average structure refinement of Cordier et al. (see Table 2 of Ref. [1]) in conjunction with the R_0 parameters from Brese and O'Keeffe [12] ($R_0(Nb^{5+}–O^{2-}) = 1.911$ Å and $R_0(Nb^{5+}–F^{-}) = 1.87$ Å, respectively), it is then possible to calculate the fractional F occupancy, x_i, for which the formal valence, $\mathrm{AV}(Xi)_{(\mathrm{ideal})}$, at each anion site, Xi, is satisfied. For example, according to the average structure refinement, the equatorial $X1$ anion is bonded to two Nb ions at a distance R of 1.9603 Å. We can therefore write

$$2 - x_1 = 2(1 - x_1)\exp[(1.911 - 1.9603)/0.37] + 2x_1 \exp[(1.87 - 1.9603)/0.37]. \quad (1)$$

Solving this equation for x_1 leads to $x_1 = 0.305$, suggesting the occupancy for the $X1$ site is 0.305 F and 0.695 O. Similar calculations performed for the $X2$, $X3$, and $X4$ anion sites results in the predicted occupancies listed in Table 2. However, if we now calculate the total number of O's and F's per unit cell, this leads to an apparent excess of oxygen (11.4 O to 8.6 F). This is not consistent with the known stoichiometry of $Nb_3O_5F_5$ (10 O, 10 F).

This result should perhaps not be unexpected since the refined average structure fractional co-ordinates (see Table 1) do not take into account the effect of 'disordered' octahedral RUM modes of distortion, the existence of which has been demonstrated in the previously presented section on electron diffraction. The effect of such octahedral rotation RUM modes is to increase slightly

Table 2
Calculated anion partial occupancies and predicted O/F composition for $Nb_3O_5F_5$ using the refined average structure [1] and without considering the presence of RUMs

Anion site	F occupancy	O occupancy	No. O/unit cell	No. F/unit cell
*X*1	0.306	0.694	5.556	2.444
*X*2	0.286	0.714	2.856	1.144
*X*3	0.836	0.164	0.6580	3.342
*X*4	0.424	0.576	2.306	1.694
Total			11.376	8.624

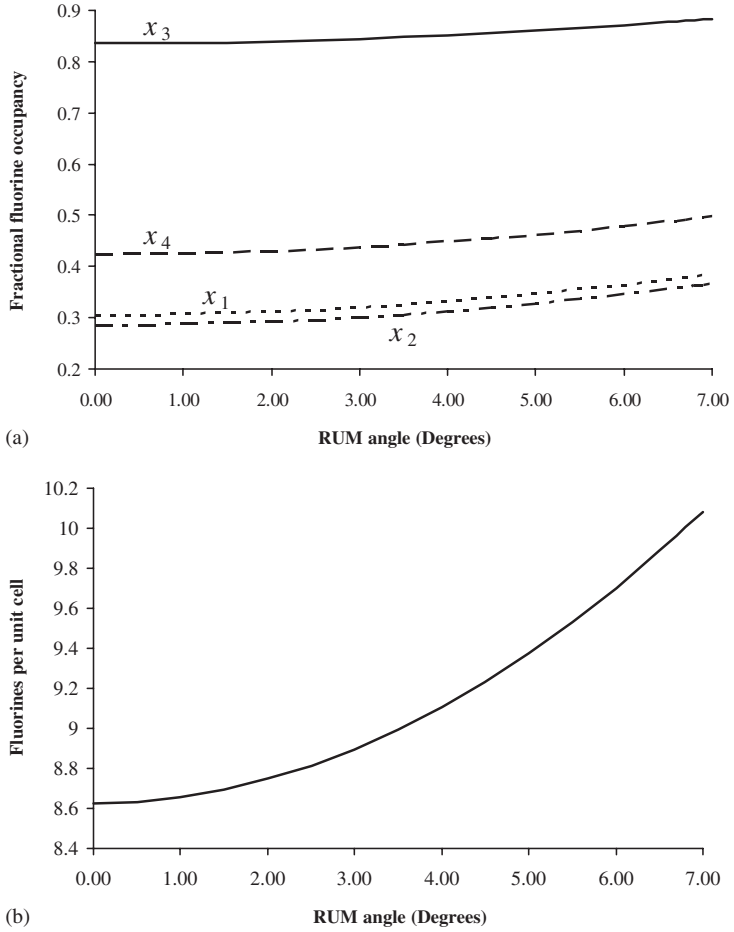

Fig. 6. (a) Graph showing the effect of RUM rotation angle, θ, on the fractional fluorine occupancy at each of the four anion sites. (b) Based on the results from (a), this graph shows the calculated fluorine content as the RUM rotation angle is varied. Note that for $Nb_3O_5F_5$ the expected stoichiometry will be 10 oxygens, 10 fluorines.

the effective Nb–*X* bond distances (see Ref. [5]). The values for the Nb–*X* bond distances used in the above calculations will therefore be in error.

Improved values for the x_i, which take into account the effect of octahedral RUM modes, were obtained as follows. The effect of the octahedral rotations was estimated by lengthening each of the Nb–*X* bond lengths equally by a factor of $1/\cos\theta$, where θ is the average magnitude of the octahedral rotation angle. The x_i were then re-calculated (see Eq. (1)) for a range of rotation angles until the correct composition was arrived at. The results of these calculations are summarized in Fig. 6. Fig. 6a displays the individual partial occupancies, x_i, at the *X*1, *X*2, *X*3, and *X*4 anion sites obtained as a function of the octahedral rotation angle. Fig. 6b then plots the corresponding total fluorine content per unit cell versus this rotation angle using the values for x_i derived from Fig. 6a.

The resultant predicted F occupancies for each of the 4 anion sites at the required overall $Nb_3O_5F_5$ stoichiometry are listed in Table 3. It can be seen that the average F

Table 3
Calculated anion partial occupancies and predicted O/F composition for $Nb_3O_5F_5$ including a RUM rotation angle of 6.8°

Anion site	F occupancy	O occupancy	No. O/unit cell	No. F/unit cell
*X*1	0.382	0.618	4.948	3.052
*X*2	0.363	0.637	2.548	1.452
*X*3	0.882	0.118	0.474	3.526
*X*4	0.494	0.506	2.024	1.976
Total			9.994	10.006

occupancy of the two equatorial anion sites (*X*1, *X*2) $= \frac{1}{3}(2 \times 0.382 + 1 \times 0.363) = 0.376$ is in rather good agreement with the occupancy deduced from the experimental diffuse distribution of 0.39. Note also that the apical *X*3 site on the border between neighboring NbO_2F-type slabs is predicted to be overwhelmingly occupied by F rather than O while the median *X*4 site within the NbO_2F-type slabs is predicted to be occupied almost 50/50 by O and F.

A rather interesting aspect of the average structure refinement by Cordier et al (see Table 2 of Ref. [1]), is the significant difference in the refined isotropic displacement parameters of the Nb1 ($B^*_{\text{equiv.}} = 1.07\,\text{Å}^2$) and Nb2 ($B^*_{\text{equiv.}} = 2.08\,\text{Å}^2$) sites, indicating the induced displacement away from the refined average position is significantly greater for the Nb2 cation than for the Nb1 cation (see Fig. 1). Given that the predicted O/F distribution for the equatorial *X*1 and *X*2 anion strings are rather similar (and hence so will be the associated induced Nb2 and Nb1 displacements along the [100] and [010] directions), this can only be true if the Nb2 ion is displaced along the ⟨001⟩ direction significantly more often than the Nb1 ion. This will be controlled by the O/F distribution along the ⟨001⟩ direction within the $n = 3$ slabs. The implication of this is that the *X*4 anions surrounding each Nb_2 cation must always be of opposite type, i.e. if one *X*4 anion is fluorine, then the other *X*4 anion should be oxygen and vice versa. The Nb_2 cation would then always be displaced along the ⟨001⟩ direction. Given the partial occupancies deduced for the apical *X*3 (0.882 F) and median *X*4 (0.504 F) anion sites, the most likely anion sequence along *c* would then be F–O–F–F or F–F–O–F (in ~77.8% of cases (i.e. $(0.882)^2$), other possibilities include F–F–O–O or O–O–F–F—10.4% (0.118×0.882), O–F–O–F or F–O–F–O—10.4%, and O–O–F–O or O–F–O–O—1.4%). The Nb2 cation would move off-center along *c* at every available site whereas the Nb1 cation would then move off-center on only 50% of the available sites (see Fig. 7). Note that if the opposing *X*4 sites were allowed to be occupied by anions of the same type, then the induced Nb1 and Nb2 cations shifts along *c* would occur with equal probability and there would be no explanation for the significantly different refined isotropic displacement parameters.

Table 4 shows the predicted occupancies of the two symmetry inequivalent anion sites of $NbOF_3$ ($n = 1$) using

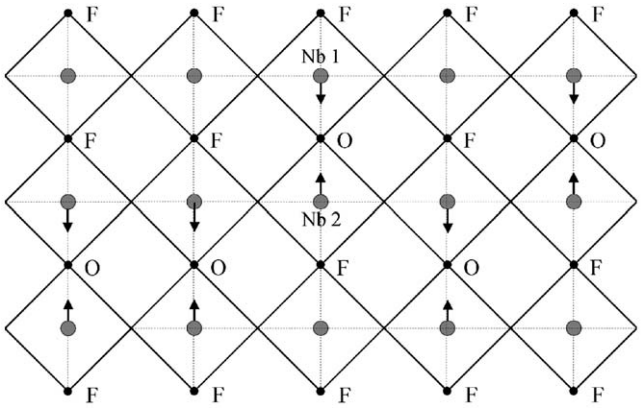

Fig. 7. Schematic diagram of likely oxygen/fluorine distribution on the apical (*X*3) and median (*X*4) anion sites. Note that, for clarity, only the most dominant (78% of cases) ordering sequences (F–O–F–F and F–F–O–F) have been shown.

Table 4
Calculated anion partial occupancies and predicted O/F composition for $NbOF_3$ including a RUM rotation angle of 7.8°

Anion site	F occupancy	O occupancy	No. O/unit cell	No. F/unit cell
*X*1	0.523	0.477	1.908	2.092
*X*2	0.977	0.023	0.092	3.908
Total			2.000	6.000

the same procedure as described above and the refined fractional co-ordinates as given in Ref. [2]. In this case the required RUM rotation angle is 7.8° (i.e. to yield the known composition of 2 O and 6 F). Again it is predicted that the apical anion site on the border between neighbouring NbO_2F-type slabs is overwhelmingly occupied by F rather than O. This is in good agreement with the conclusions reached by Köhler et al. [2]. Note that in this case the position of the diffuse sheets perpendicular to **a** and **b** would be expected to be close to $q = 0.5$.

In conclusion, it is clear from this investigation of $Nb_3O_5F_5$ that O^{2-} and F^- ions are again ordered in one-dimensional strings along *a* and *b*, without there being any correlation from one such string to the next. There is also indirect evidence to suggest that short range O/F ordering also occurs along **c**, within the NbO_2F slabs. Due to the relative $\frac{1}{2}\mathbf{a} + \frac{1}{2}\mathbf{b}$ shear type displacement between the NbO_2F slabs, however, this does not lead to long range ordering of the O and F anions along the **c** direction and hence to an observable (diffuse scattering type) diffraction effect. Bond valence sum calculations performed on $NbOF_3$ ($n = 1$) predict an analogous pattern of O/F ordering along **a** and **b** strongly suggesting that such one-dimensional O/F ordering is common to the entire family of $Nb_nO_{2n-1}F_{n+2}$ oxyfluorides.

Acknowledgments

RLW thanks the Australian Research Council (ARC) for financial support in the form of an ARC Discovery grant.

References

[1] S. Cordier, T. Roisnel, M. Poulain, J. Solid State Chem. 177 (2004) 3120.
[2] J. Köhler, A. Simon, L. van Wüllen, S. Cordier, T. Roisnel, M. Poulain, M. Somer, Z. Anorg. Allg. Chem. 628 (2002) 2683.
[3] L.K. Frevel, H.W. Rinn, Acta Crystallogr. 11 (1956) 54.
[4] A.W. Sleight, Inorg. Chem. 8 (1969) 1764.
[5] F.J. Brink, R.L. Withers, L. Norén, J. Solid State Chem. 166 (2002) 73.
[6] B.D. Butler, T.R. Welberry, Acta Crystallogr. A 49 (1993) 736.
[7] B.D. Butler, R.L. Withers, T.R. Welberry, Acta Crystallogr. A 48 (1992) 737.
[8] M.P. Crosnier-Lopez, N.S.P. Bhuvanesh, H. Duroy, J.L. Fourquet, J. Solid State Chem. 145 (1999) 136.
[9] F.J. Brink, L. Norén, R.L. Withers, J. Solid State Chem. 177 (2004) 2177.
[10] M. Zakhour-Nakhl, J.B. Claridge, J. Darriet, F. Weill, H.-C. Zur Loye, J.M. Perez-Mato, J. Am. Chem. Soc. 122 (2000) 1618.
[11] H.-C. zur Loye, M.D. Smith, K.E. Stitzer, A. El Abed, J. Darriet, MRS Symp. Proc. GG1.4.1. (2001) 658.
[12] N.E. Brese, M. O'Keeffe, Acta Crystallogr. B 47 (1991) 192.